-RXUQDO RI 0HPEUDQH 6FLHQFH 5HVH

MRXUQDO KRPHSDJH ZZZ PVUMRXUQDO FRP

Research Paper

0RGHOLQJ DQG ([SHULPHQWDO 6WXG\ RI &DUERQ 'LR[Contactor

1D\HI *KDVHP 0RKDPHG $O 0DU]RXTL

'HSDUWPHQW RI &KHPLFDO 3HWUROHXP (QJLQHHULQJ 8$(8QLYHUVLW\ $O $LQ FLW\ 8QLW

ARTICLE INFO

Received 2016-03-21
Revised 2016-06-14
Accepted 2016-06-14
Available online 2016-06-14

GRAPHICAL ABSTRACT

KEYWORDS

CO_2 absorption
Membrane contactor
Flat sheet
Modeling and simulations

HIGHLIGHTS

‡ 39') ÀDW VKHHW PHPEUDQH LV HPSOR\HG IRU WKH DEVRUSWLRQ RI &2
‡ $TXHRXV VRGLXP K\GUR[LGH VROXWLRQ LV XVHG DV WKH DEVRUEHQW OLTXLG
‡ :H GHYHORSHG D ' PDWKHPDWLFDO PRGHO WR GHVFULEH WKH SURFHVV DQG VROYHG E\ &2062/
‡ 7KH HuHFW RI 1D2+ FRQFHQWUDWLRQ DQG LQOHW JDV DQG OLTXLG UDWH RQ VHSDUDWLRQ ZDV VWXG
‡ 7KH PRGHO SUHGLFWLRQV ZHUH LQ JRRG DJUHHPHQW ZLWK H[SHULPHQWDO GDWD

ABSTRACT

,Q WKH SUHVHQW VWXG\ &2 QDWXUDO JDV VWUHDP KDV EHHQ VWXGLHG XVLQJ D ÀDW VKHHW PHPEUDQ
WKH SURFHVV 7KH PRGHO FRQVLGHUV WKH WUDQVSRUW RI D JDV PL[WXUH FRQWDLQLQJ FDUERQ GLR
WKH QRQ ZHWWHG PRGH RI RSHUDWLRQ LQ ZKLFK WKH JDV ¿OOV WKH PHPEUDQH SRUHV LQ D FRXQWH
&)' RI WKH PRGHO PDWHULDO DQG PRPHQWXP WUDQVSRUW HTXDWLRQV LQ WKH ÀDW VKHHW PHPEUDQ
VLPXODWLRQV IRU WKH DEVRUSWLRQ RI &2 LQ VRGLXP K\GUR[LGH VROXWLRQ 6LPXODWLRQ SUHGLFWLRQV ZHUH LQ
ÀRZ UDWHV 7KH PRGHOLQJ SUHGLFWLRQV LQGLFDWHG WKDW WKH UHPRYDO RI &2 LQFUHDVHG ZLWK LQFUHDVLQJ WKH OLTXLG ÀRZ UDWH DQG LQF
JDV ÀRZ UDWH KDV QHJDWLYH HuHFW

,QWURGXFWLRQ

*OREDO ZDUPLQJ LV FDXVHG E\ WKH HPLVVLRQ RI JUHHQKRXVH JDVHV VXFK DV &2 GLR[LGH &2 WKH SULPDU\ JUHHQKRXVH JDV activities > @ 7KHUHIRUH WKHUH LV D GH¿QLWH QHHG WR GHYHORS FRVW HIIHFWLYH DQG QRYHO VHSDUDWLRQ SURFHVVHV IRU &2 UHPRYDO 7KH FRQYHQWLRQDO DEVRUSWLRQ SURFHVVHV DUH ODUJH LQ VL]H DQG UHTXLUH KLJK RSHUDWLRQDO OLPLWDWLRQV OLTXLG ÀRRGLQJ PHPEUDQH FRQWDFWRU KDV EHHQ DWWUDFWHG

> @8VLQJ D PHPEUDQH FRQWDFWRU takes place in WKH JDV SKDVH ... [overlapping, illegible]

&RUUHVSRQGLQJ DXWKRU DW 3KRQH ID[
(PDLO DGGUHVV 1 *KDVHP

DOI: 10.22079/jmsr.2016.20226

and foaming problems which may take place in the traditional packed columns. A comprehensive review of the developments in membrane-based technologies for CO_2 capture was covered by Luis et al. [8]. The research on CO_2 capture from flue gas and natural gas using gas-liquid hollow fiber membrane contactor has been studied by a number of researchers [9–19].

Various mathematical models have also been proposed to describe the capture of CO_2 from gas mixture using gas-liquid hollow fiber membrane contactors. The models were validated with experimental results to verify and predict the consequences of varying operating parameters and structure of hollow fiber membranes on contactor absorption performance. A mathematical model that describes the SO_2 absorption in hollow fiber ceramic membrane contactor was developed by Luis et al. [20]. Several other numerical models were developed to describe the influence of membrane wetting on CO_2 capture in hollow fiber membrane contactor. These models were based on resistance-in-series [21-23]. Moreover, the influence of pore size, pore size distribution and effective surface porosity on membrane mass transfer coefficient was studied by Li et al. [24]. Mavroudi et al. [25] studied the membrane resistance change with time of physical absorption of pure CO_2. Gas liquid membrane contactor can also be used for stripping CO_2 from amine solution [26]. However, most of the mathematical models focused on hollow fiber membrane contactor. To the best of our knowledge none was developed for flat sheet membrane contactor using three dimensional (3D) approach for the absorption of CO_2 from natural gas using aqueous NaOH solvent.

The aim of the present work was to develop a 3D mass transfer model for absorption of CO_2 from natural gas in a flat sheet membrane contactor. Aqueous NaOH solution is considered as the chemical solvent in simulations. Computational fluid dynamic technique is used for numerical simulation, and results of simulations are then compared with experimental data. The experimental work was performed via microporous PVDF flat sheet membrane casted through thermally induced phased separation (TIPS) technique. The in-lab made PVDF flat sheet membrane contactor modules were used in the absorption of CO_2 from a gas mixture that consists of 10% CO_2/90%CH_4 through a 0.5 M NaOH solution.

2. Model development

Material and momentum transport equations were considered in the development of the mathematical model. The proposed model describes the transport of gas mixture and liquid solvent in a countercurrent flat sheet membrane contactor [27-29]. The steady state model equations developed for module segment are shown in Figure 1.

2.1. Gas phase

The steady state continuity equation is used for the prediction of carbon dioxide concentration in the gas phase:

$$v_{y\text{-}g}\frac{\partial C_i}{\partial y}=D_{i\text{-}g}\left[\frac{\partial^2 C_{i\text{-}g}}{\partial x^2}+\frac{\partial^2 C_{i\text{-}g}}{\partial y^2}+\frac{\partial^2 C_{i\text{-}g}}{\partial z^2}\right] \quad (1)$$

where v_{y-g} refers to the velocity of the gas phase in y-direction, $C_{i\text{-}g}$ is the concentration of carbon dioxide in gas phase along the length of the membrane. The model is built up for non-wetting mode of operation (i.e. gas filled pores). Under countercurrent mode of operation, the following boundary conditions exist:

$z=z_2,\ C_{i,g}=C_{i,m}$ identical concentration at the membrane-gas interface (2)

$z=z_3,\ -\frac{\partial C_{i,s}}{\partial x}=0$ module walls (3)

$y=0,\ -\frac{\partial C_{i,g}}{\partial x}=0$ Convective flux, outlet of gas stream (4)

$y=L,\ C_{CO_2,g}=C^{\circ}_{CO_2},\ C_{CH_4,g}=C^{\circ}_{CH_4}$ inlet gas stream (5)

$x=0$ and $x=w;\ \frac{\partial C_{i,g}}{\partial x}=0$ membrane module side walls (6)

The velocity distribution in the gas phase is calculated using Navier-Stokes equation.

$$\rho\left(\frac{\partial u}{\partial t}+u\frac{\partial u}{\partial x}+v\frac{\partial u}{\partial y}+w\frac{\partial u}{\partial z}\right)=\rho g_x-\frac{\partial p}{\partial x}+\mu\left(\frac{\partial^2 u}{\partial x^2}+\frac{\partial^2 u}{\partial y^2}+\frac{\partial^2 u}{\partial z^2}\right) \quad (7)$$

Boundary conditions for the Navier-stokes equations may be written as:

$y=L;\ u=u_0$ inlet gas velocity (8)

$y=0;\ P=P_{atm}$ gas outlet stream (9)

$z=z_2;\ u=0$ membrane-gas interface (10)

$z=z_3;\ u=0$ gas chamber top wall (11)

$x=0; x=w; u=0$ module side walls (12)

where u is the velocity in the y-direction, L is the length of membrane, w is the width of the membrane.

2.1.2. Membrane section

The steady-state material balance for the transport of CO_2 and CH_4 along the membrane thickness for non-wetting mode of operation is considered to be due to diffusion only; no reactions are taking place in the gas filled pores (i = CO_2 and CH_4).

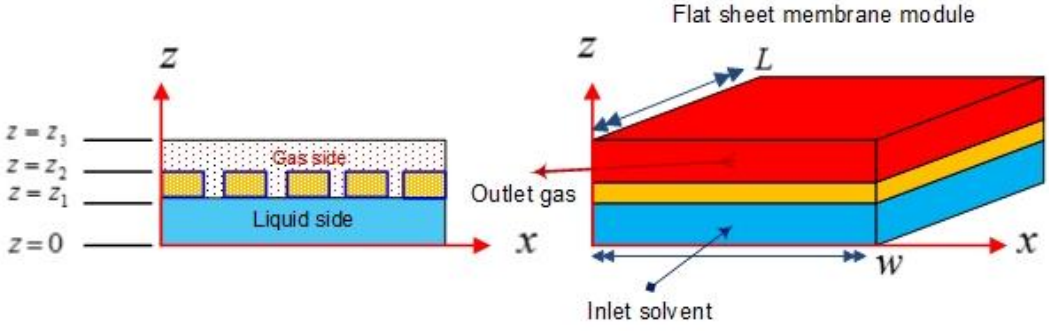

Fig. 1. Schematic diagram of flat sheet membrane contactor used for CO_2 capture.

$$D_{i,m}\left[\frac{\partial^2 C_{i,m}}{\partial x^2}+\frac{\partial^2 C_{i,m}}{\partial y^2}+\frac{\partial^2 C_{i,m}}{\partial z^2}\right]=0 \quad (13)$$

Boundary conditions:

$z=z_1,\ C_{i,m}=C_{i,l}/m_i$ membrane-liquid interface (14)

$z=z_2,\ C_{i,m}=C_{i,l}$ membrane-gas interface (15)

$y=0,\ y=L,\ \frac{\partial C_{i,m}}{\partial z}=0$ Thermal insulation at both ends of membrane walls (16)

$x=0$ and $x=w;\ \frac{\partial C_{i,m}}{\partial y}=0$ membrane walls (17)

where m_i is the solubility CO_2 and CH_4 in aqueous sodium hydroxide solution.

2.1.3. Liquid side

The steady-state material balance for the transport of CO_2 and aqueous NaOH in the liquid side of the flat sheet membrane is considered to be due to diffusion, convection and reaction as well. The reaction overall rate can be determined depending on its mechanisms and reaction rates. The right hand side of the following equation represents the diffusion and reaction terms, whereas the left hand side of the equation is the convective term [20-22].

$$v_{y\text{-}l}\frac{\partial C_i}{\partial y}=D_{i\text{-}l}\left[\frac{\partial^2 C_{i\text{-}l}}{\partial x^2}+\frac{\partial^2 C_{i\text{-}l}}{\partial y^2}+\frac{\partial^2 C_{i\text{-}l}}{\partial z^2}\right]+r_i \quad (18)$$

where the subscript "*i*" indicates carbon dioxide and sodium hydroxide. Reaction rates for CO_2 and NaOH are shown in equations 20 and 21, respectively:

$$2NaOH+CO_2\rightarrow Na_2CO_3+H_2O \quad (19)$$

$$r_{CO_{2,t}}=-k_r C_{CO_2,l}C_{NaOH,l} \quad (20)$$

$$r_{NaOH,t}=-2k_r C_{CO_2,l}C_{NaOH,l} \quad (21)$$

Boundary conditions:

The boundary conditions for solvent flowing in liquid compartment of the flat sheet membrane are shown below (i = CO_2 and NaOH):

$z=z_1,\ C_{i,l}=m_i C_{i.m}$ gas solubility in solvent at liquid-membrane interface (22)

$z=0,\ -\frac{\partial C_{i,l}}{\partial z}=0$ module wall (23)

$y=0,\ C_{NaOH,l}=C^{\circ}_{NaOH}$ solvent initial feed concentration (24)

$y=L,\ \frac{\partial C_{i,l}}{\partial y}=0$ liquid exit stream (25)

$x=0,\ x=w;\frac{\partial C_{i,l}}{\partial y}=0$ module left and right side walls (26)

The velocity distribution in the liquid phase is calculated using Navier-Stokes equations:

$$\rho\left(\frac{\partial u}{\partial t}+u\frac{\partial u}{\partial x}+v\frac{\partial u}{\partial y}+w\frac{\partial u}{\partial z}\right)=\rho g_x-\frac{\partial p}{\partial x}+\mu\left(\frac{\partial^2 u}{\partial x^2}+\frac{\partial^2 u}{\partial y^2}+\frac{\partial^2 u}{\partial z^2}\right) \quad (27)$$

Boundary conditions for the Navier-stokes equations can be written as:

$y=0;\ u=u_0$ inlet liquid velocity (28)

$y=L;\ P=P_{atm}$ liquid side outlet flow (29)

$z=0;\ u=0$ liquid side bottom wall (30)

$z=z_1;\ u=0$ liquid-membrane interface (31)

$x=0; x=w; u=0$ liquid chamber left and right side walls (32)

Model parameters are shown in Table 1. Physical properties such as density and viscosity as a function of temperature and pressure are built in COMSOL software, for the absorbent liquid, the property of water is being assumed.

Table 1
Numerical values of the parameters used for modeling.

Parameter	Value	Reference
$d(m)$	0.0025	Measured
$W(m)$	0.04	Measured
$L(m)$	0.09	Measured
$D_{CO_2,gas}(m^2/s)$	1.855×10^{-5}	[30]
$D_{CO_2,liq}(m^2/s)$	$2.35\times10^{-6}\exp(-2119/T)$	[31]
$D_{CO_2-mem}(m^2/s)$	$(\varepsilon/\tau)\times D_{CO_2,gas}$	Estimated
$D_{Solv,liq}(m^2/s)$	$0.5\times D_{CO_2,liq}$	Estimated
m_{CO_2}	$3.59\times10^{-7}RT\exp(2044/T)$	[31]
$k_r\left(m^3/mol.s\right)$	$10^{11.916-2382/T}/1000$	[33]
Membrane porosity, ε	0.17	Measured
Tortuosity, τ	$(2-\varepsilon)^2/\varepsilon$	[32]

3. Experimental work

3.1. Materials

Poly (vinylidene fluoride) (PVDF) (Solef® 6020/1001) was purchased from Solvay company, France. Glycerol triacetate (triacetin), ethanol and sodium hydroxide were purchased from Sigma-Aldrich; all materials were with purity more than 99%. All chemicals were used as received without further purification. Gas mixture (e.g. 10 vol% CO_2, 90 vol% CH_4) cylinder was purchased for Air Product (UAE). Two types of epoxy were used: at room temperate, Araldite 5 minutes rapid, Belgium. For high temperature Emerson Stycast 2651W-Catalyst 9 (operating temperature: -40 to 130 °C) was purchased from Ellsworth Adhesive Ltd. (UK).

3.2. Preparation of flat sheet membrane module

Various polymeric flat sheet membranes were casted for CO_2 removalfrom CO_2/CH_4 gas mixture. Polyether sulfone (PES) and Polyvinylidene fluoride (PVDF) were used for fabricating the flat sheet membranes. Selected amount of polymer was mixed with *N, N*-Dimethylacetamide (DMAc) in ratio of 1:4. The PES mixture was kept overnight in order to produce homogenous mixture at room temperature. By contrast, heating is used for the preparation of PVDF/DMAc dope solution. The homogenous transparent dope solution was then spread on a Pyrex glass and it was balanced from all edges using casting machine in order to get a uniform thickness. The Pyrex glass along with the dope solution was then immersed in deionized water at room temperature for one day. The solvent is transferred into water and the dope mixture is agglomerated and formed polymeric flat sheet membrane. The membrane was then drayed in a freeze dryer in order to remove any moisture left. Afterward, it was cut to 4 × 9 cm to fit with the exact available space in the flat sheet module.

3.3. Gas absorption

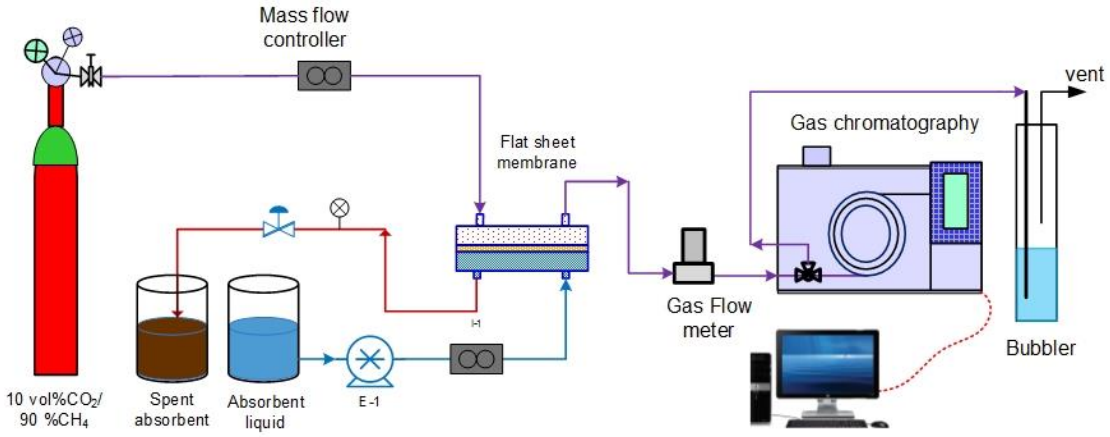

Fig. 2. Experimental setup used for CO_2 absorption experiments.

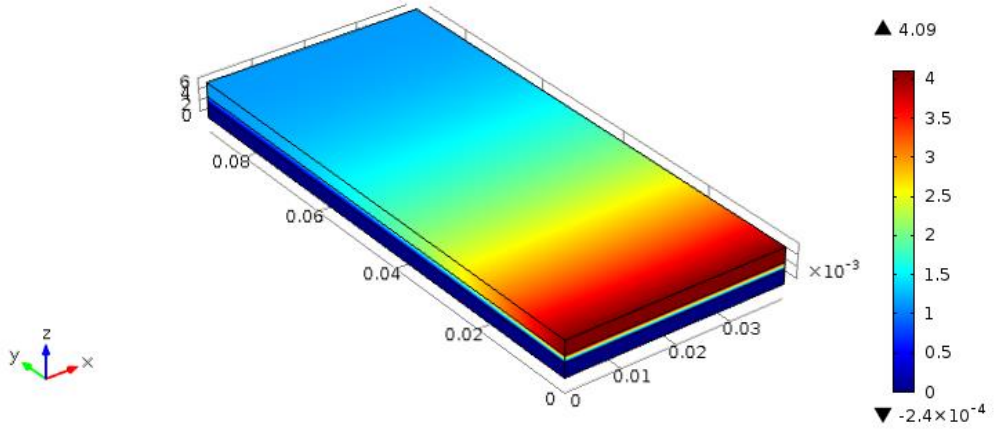

Fig. 3. Surface plot (3D) of carbon dioxide concentration in flat sheet membrane generated with COMSOL 5.1.

The schematic diagram of the experimental setup used in CO_2 absorption is shown in Figure 2. The experimental setup consists of a flat sheet module (consists of two compartments separated by flat sheet polymeric membrane). Gas and liquid streams enters the module in countercurrent flow. Flow rates are controlled by mass flow controllers (Alicat, USA). The solvent (NaOH) flow rate is adjusted through a peristaltic pump (Masterflex, USA). The effect of inlet absorbent temperature on system performance was investigated. The gas free water vapor is sent to the gas chromatography (Shimadzu, Japan). The gas chromatography analysis is used to measure the CO_2 concentration in the exit gas stream. The experimental operating conditions are shown in Table 2.

Table 2
The operating conditions used in the absorption experiments, at 1 atm.

Inlet liquid flow rate, $(ml/\min)$	10
Inlet gas flow rate, $(ml/\min)$	100
Inlet liquid temperatures, (^oC)	25
Inlet gas temperature, (^oC)	25

4. Results and discussion

A mathematical model for the transport of CO_2 through the proposed PVDF flat sheet membrane contactor module has been developed with aqueous NaOH as the absorbent liquid. Non-wetting mode of operation is considered. The model equations were solved using COMSOL 5.1. The computational time for the simulation is 14 seconds using computer Intel CORE i7. The model prediction of surface plot for carbon dioxide concentration across the membrane is shown in Figure 3. The model equations were solved for investigating the effect of gas and liquid flow rates, solvent temperatures and various NaOH concentration on membrane performance. The objective of simulation is to study the effect of operational conditions on the system performance, i.e. the percent of CO_2 removal. By assuming equal inlet and outlet gas streams, the amount of removed CO_2 does not affect the gas flow rate [8].

$$\eta = \frac{C_{CO_2,in} - C_{CO_2,out}}{C_{CO_2,in}} \tag{33}$$

The CO_2 removal flux

$$J_{CO_2} = \frac{Q_{in}\left(C_{CO_2,in} - C_{CO_2,out}\right)}{A_s} \tag{34}$$

where J_{CO_2} is the removal flux of CO_2 $(mol/m^2 s)$, A_s is the total membrane area (m^2), Q_{in} is the gas volumetric flow rates (m^3/h) and $C_{CO_2,in}$ and $C_{CO_2,out}$ are the CO_2 molar concentrations in the gas phase (mol/m^3) at the inlet and outlet streams, respectively. Moreover, η refers to the CO_2 removal fraction. Since the maximum CO_2 concentration of the inlet gas mixture is very low, the change in volumetric flow rate is assumed to be negligible. Thus removal efficiency can be approximated by Eq. (33). The exit gas concentration ($C_{CO_2,out}$) is derived by means of surface average. The removal flux is calculated by Eq. (34). Concentration distribution of CO_2 in the gas phase is the most important parameter for optimization of process. Decreasing CO_2 concentration in the gas phase determines the CO_2 removal rate. The surface plot of the concentration of CO_2 in the liquid, membrane and gas compartments of the membrane contactor module are shown in Figure 3. The gas mixture flows into the gas side of the contactor (at y = *L*) where the concentration of CO_2 is the highest. On the other hand, NaOH solution flows into the liquid compartment side (at y = 0), where the concentration of CO_2 is assumed to be zero. As the gas flows through the gas compartment side, it diffuses through the membrane pores due to the concentration gradient. The

penetrated CO_2 to the liquid side is absorbed by the flowing solvent, where it reacts and gets consumed. In the liquid and gas compartments, the flux vectors are in both the *x* and the *y* directions. This is due to convection and diffusion; whereas within the membrane, the flux vectors are in two *z*-directions due to diffusion only. In the membrane side, only diffusion is taking place.

4.1. Axial concentration profile

The axial concentration of CO_2 along the gas-membrane interface is illustrated in Figure 4. The CO_2 concentration decreases along the gas-membrane interface till it reaches the minimum value at the outlet of the membrane contactor module. This is attributed to the consumption of carbon dioxide along the length of the membrane due to the progress in reaction rate.

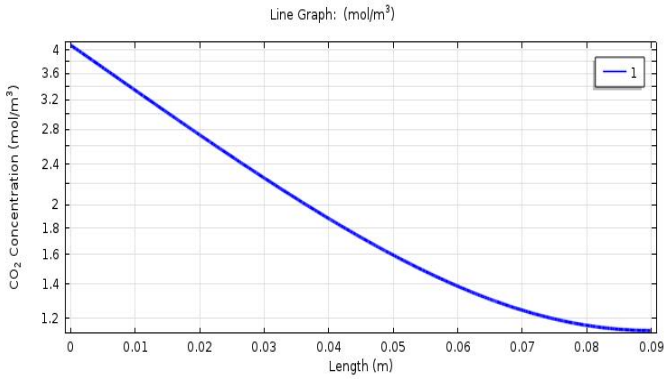

Fig. 4. Predicted axial CO_2 concentration profile at tube-membrane interface along membrane length.

4.2. Model validation

The 3D mathematical model was solved using COMSOL 5.1 software package. The modeling predictions for the physical and chemical absorption of 10% CO_2 in the 0.5 M aqueous sodium hydroxide solvent (using a flat sheet PVDF membrane contactor) are compared with the experimental data. The membrane geometry and operating parameters used in the simulation are shown in Table 1. The experimental uncertainty in the experimental data is ± 2.3%. As could be observed in Figure 5, the model predictions are in good agreement with the experimental data at different values of inlet gas flow rate in the module. It is worth quoting that an average deviation of less than 10% was calculated between experimental and simulation results.

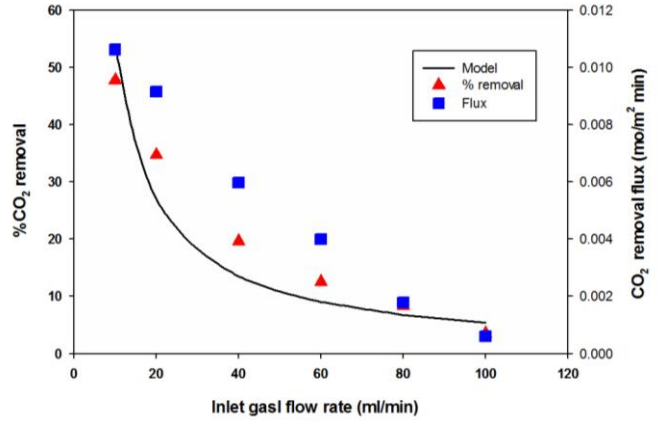

Fig. 5. Comparison of modeling predictions (solid line) and experimental data (triangle) for the percent CO_2 removal and (square) for CO_2 removal flux at variable inlet gas flow rate in the module.

4.3. Effect of aqueous NaOH concentration

The experimental data for the effects of solvent concentration on removal efficiency and removal flux are illustrated in Figures 6 and 7, respectively. As could be observed, increasing the solvent concentration improves the removal efficiency and the removal flux of CO_2. This is attributed to the fact that the active absorption of carbon dioxide at liquid boundary layer is increased with increasing solvent concentration. Since the reaction rate is a function of the CO_2 and NaOH concentrations, an increasing in NaOH concentration enhances the reaction rate. As a consequence, it increases the consumption rate of carbon dioxide.

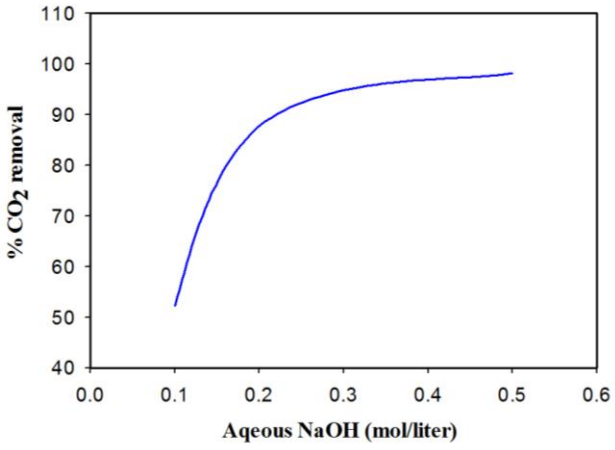

Fig. 6. Effect of aqueous NaOH concentration on the percent of CO_2 removal.

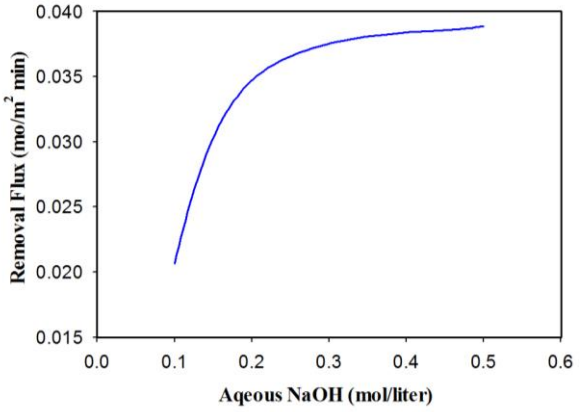

Fig. 7. Effect of aqueous NaOH concentration on the CO_2 removal flux.

4.4. Effect of gas temperature

The effect of inlet gas temperature on the membrane performance was also investigated. Results revealed that CO_2 removal efficiency for different values of inlet gas temperature has almost no significant effect on the carbon dioxide removal process (see Figure 8).

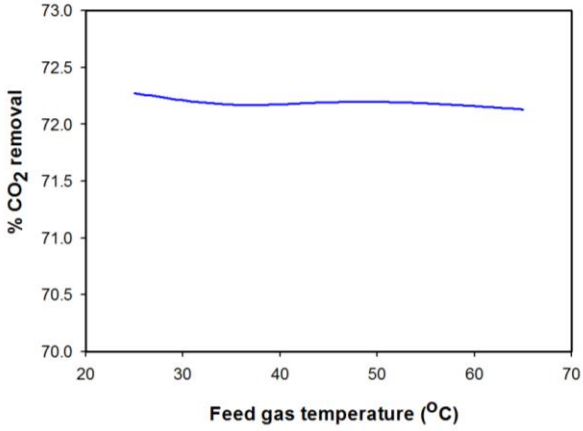

Fig. 8. Effect of inlet gas temperature on the percent removal of CO_2.

4.5. Effect of gas flow rate

The effect of inlet gas flow rate on the CO_2 removal efficiency is performed experimentally (see Figure 9). As could be observed, the removal efficiency decreases with increasing gas flow rate. The increase in the gas flow rate reduces the residence time in the membrane contactor, which in turn decreases the CO_2 removal rate. The percentage removal of CO_2 decreases from 50% to 5% when the gas flow rate, in the flat sheet membrane, changes from 10 ml/min to 100 ml/min. Also the figure specifies that gas flow rate affects the CO_2 removal rate in the gas-liquid flat sheet membrane contactor to certain extent.

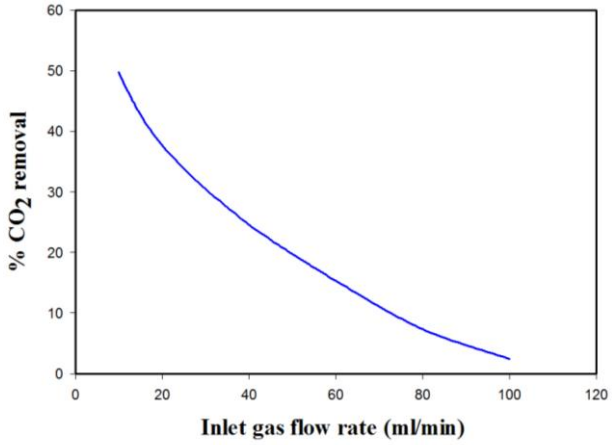

Fig. 9. Effect of inlet gas flow rate on the percentage removal of CO_2.

4.6. Effect of liquid temperature

The variation in solvent temperature affects the reaction rate constant and the solubility of the CO_2 in solvent, as well. As a result, the change in temperature is expected to cause significant impact on the rate of CO_2 absorption. Figure 10 shows experimentally the effect of temperature on the CO_2 percent removal. As can be seen, with increasing solvent temperature, the CO_2 removal rate also increases. This can be attributed to the fact that as the temperature increases, the reaction rate increases due to increase in reaction rate constant and, consequently, more CO_2 is absorbed. The physical solubility decreases with temperature; meanwhile the chemical solubility increases with temperature, which leads to the increase in the percent of CO_2 removal. A net enhancement of CO_2 removal is also observed with increasing temperature.

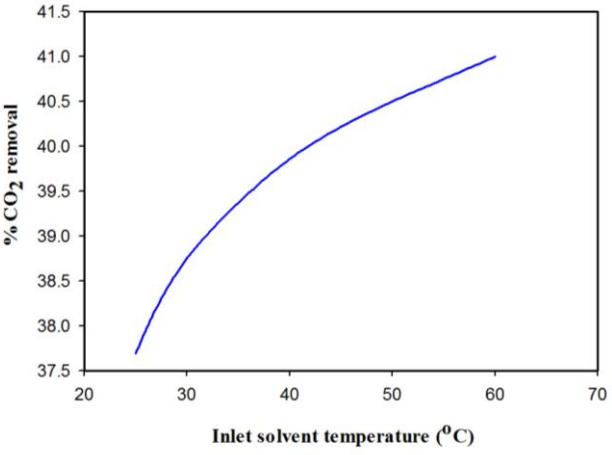

Fig. 10. Effect of solvent temperature on the percentage removal of CO_2.

4.7. Effect of liquid flow rate

Figure 11 illustrates the experimental results for the variation of the percentage removal of CO_2 as a function of liquid flow rate. As the absorbent flow rate increases, the mass transfer rate of carbon dioxide into the liquid increases due to the concentration gradients of CO_2 and absorbent in the liquid increase. Thus the CO_2 outlet concentration in gas decreases and the percentage removal of CO_2 increases [34]. The figure clearly indicates that liquid flow rate in the flat sheet membrane has significant effect on the CO_2 removal.

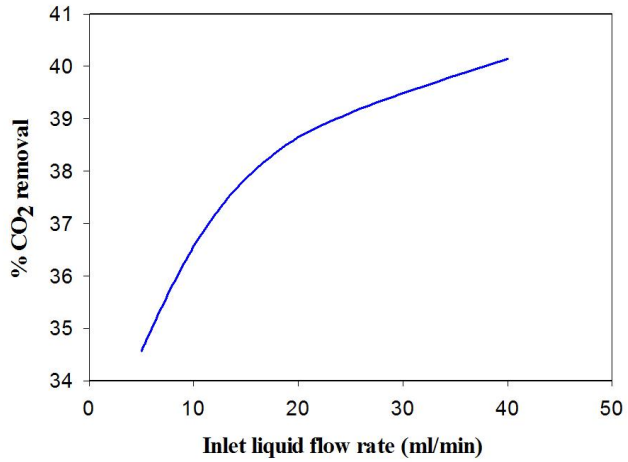

Fig. 11. Effect of inlet liquid flow rate on the percentage removal of CO_2.

5. Conclusions

Flat sheet membranes offer moderate membrane surface/volume ratios compared to hollow fiber membranes. A mathematical model was developed to describe the transport of CO_2 in a flat sheet membrane contactor using aqueous NaOH as the absorbing agent. The model was established considers non-wetting condition for a countercurrent gas–liquid flow arrangement. The model was validated with experimental data. The model predictions and experimental data were in good agreement. The effect of solvent concentrations, gas and liquid flow rates, liquid temperature on the CO_2 removal efficiency and removal flux were studied. The removal percentage of CO_2 was found to increase with increasing the NaOH concentration. Both liquid temperature and liquid flow rate encouraged the removal process. By contrast, gas flow rate can has a negative effect.

6. Nomenclature

A	Total area of membrane, m^2
C_i	Concentration of component i ; 1: CO_2, 2: CH_4, 3: NaOH
$C_{i,m}$	Concentration of component i in the membrane section, mol m^{-3}
$C_{i,g}$	Concentration of component i in the gas section, mol m^{-3}
$C_{i,l}$	Concentration of component i in the liquid section, mol m^{-3}
D_i	Diffusion coefficient of component i : 1: CO_2, 2: CH_4, 3: NaOH
L	Length module, m
W	Module width, m
m	Physical solubility

Greek letters

ρ	Gas density, g cm^{-3}
μ	Viscosity of gas, Pa s
ε	Membrane bulk porosity

7. References

[1] N. Abdul Rahim, N. Ghasem, M. Al-Marzouqi, Absorption of CO_2 from natural gas using different amino acid salt solutions and regeneration using hollow fiber membrane contactors. J Nat. Gas Sci. Eng. 26 (2015) 108-117.

[2] N. Ghasem, M. Al-Marzouqi, Z. Ismail, Gas–liquid membrane contactor for ethylene/ethane separation by aqueous silver nitrate solution, Sep. Purif.

Technol. 127 (2014) 140–148.
[3] Y. Le Moullec, T. Neveux, A. Al Azki, A. Chikukwa, K. A. Hoff, K, Process modifications for solvent-based post-combustion CO_2 capture. Int. J. Greenh. Gas Con. 31 (2014) 96–112.
[4] S.M.R. Razavi, S.M.J Razavi, T. S. Miri, Shirazian, CFD simulation of CO_2 capture from gas mixtures in nanoporous membranes by solution of 2-amino-2-methyl-1-propanol and piperazine. Int. J. Greenh. Gas Con. 15 (2013), 142–149.
[5] S. Shirazian, S.N. Ashrafizadeh, Mass transfer simulation of carbon dioxide absorption in a hollow-fiber membrane contactor. Sep. Sci. Technol. 45 (2010), 515–524.
[6] S. Shirazian, A. Marjanm, F. Azizmohammadi, Prediction of SO_2 transport across ceramic membranes using finite element method (FEM). Orient. J. Chem. 27 (2011), 485–490.
[7] A. Gabelman, S.T., Huang, Hollow fiber membrane contactors. J. Membr. Sci. 159 (1999) 61–106.
[8] P. Luis, T. V. Gerven, B. V. der Bruggen, Recent developments in membrane-based technologies for CO_2 capture, Prog. Energy Combust. Sci. 38 (2012) 419-448.
[9] N.M. Ghasem, M. Al-Marzouqi, A. Duaidar, Effect of quenching temperature on the performance of poly (vinylidene fluoride) microporous hollow fiber membranes fabricated via thermally induced phase separation technique on the removal of CO_2 from CO_2 - gas mixture, Int. J. Greenh. Gas Cont. 5 (2011) 1550–1558.
[10] P. Luis, B. V. der Bruggen, T. V. Gerven, Non-dispersive absorption for CO_2 capture: from laboratory to industry, J. Chem. Technol. Biotechnol. 86 (2011) 769-775.
[11] Y.-S. Kim, S.-M. Yang, Absorption of carbon dioxide through hollow fiber membranes using various aqueous absorbents, Sep. Purif. Technol. 21 (2000) 101–109.
[12] V.Y. Dindore, D.W.F. Brilman, F.H. Geuzebroek, G.F. Versteeg, Membrane solvent selection for CO_2 removal using membrane gas–liquid contactors, Sep. Purif. Technol. 40 (2004) 133-145.
[13] E. Drioli, A. Criscuoli, E. Curcio, Membrane contactors: fundamentals, applications and potentialities, Vol. 11, Elsevier, DEC-2005.
[14] N. M. Ghasem, M. Al-Marzouqi, N. Abdul Rahim, Effect of polymer extrusion temperature on poly(vinylidene fluoride) hollow fiber membranes: Properties and performance used as gas–liquid membrane contactor for CO_2 absorption, Sep. Purif. Technol. 99 (2012) 91–103.
[15] N. M. Ghasem, M. Al-Marzouqi, L.P. Zhu, Preparation and properties of polyether sulfone hollow fiber membranes with o-xylene as a additive used in membrane contactors for CO_2 absorption, Sep. Purif. Technol. 12 (2012) 1-10.
[16] S. Atchariyawut, R. Jiraratananon, R. Wang, Separation of CO_2 from CH_4 by using gas–liquid membrane contacting process, J. Membr. Sci. 304 (2007) 163–172.
[17] M. Hedayat, M. Soltanieh, S.A. Mousavi, Simultaneous separation of H_2S and CO_2 from natural gas by hollow fiber membrane contactor using mixture of alkanolamines, J. Membr. Sci. 377 (2011) 191–197.
[18] R. Wang, H.Y. Zhang, P.H.M. Feron, D.T. Liang, Influence of membrane wetting on CO_2capture in microporous hollow fiber membrane contactors, Sep. Purif. Technol. 46 (2005) 33–40.
[19] N. Abdul Rahim, N. Ghasem, M. Al-Marzouqi, Absorption of CO_2 from natural gas using different amino acid salt solutions and regeneration using hollow fiber membrane contactors. J Nat. Gas Sci. Eng. 26 (2015) 108-117.
[20] P. Luis, A. Garea, A. Irabien, Modeling of a hollow fiber ceramic contactor for SO_2 absorption, Sep. Purif. Technol. 72 (2010) 174-179.
[21] S. Khaisri, D. deMontigny, P. Tontiwachwuthikul, R. Jiraratananon, A mathematical model for gas absorption membrane contactors that studies the effect of partially wetted membranes, J. Membr. Sci. 347 (2010) 228–239.
[22] J.-G. Lu, Y.-F. Zheng, M.-D. Cheng, wetting mechanism in mass transfer process of hydrophobic membrane gas absorption, J. Membr. Sci. 308 (2008) 180–190.
[23] S. Atchariyawut, R. Jiraratananon, R. Wang, Mass transfer study and modeling of gas–liquid membrane contacting process by multistage cascade model for CO_2 absorption, Sep. Purif. Technol. 63 (2008) 15–22.
[24] K. Li, J. Kong, X. Tan, Design of hollow fiber membrane modules for soluble gas removal, Chem. Eng. Sci. 55 (2000) 5579–5588.
[25] M. Mavroudi, S.P. Kaldis, G.P. Sakellaropoulos, A study of mass transfer resistance in membrane gas–liquid contacting processes, J. Membr. Sci. 272 (2006) 103–115.
[26] Z. A. Tarsa1, S. Ali Asghar Hedayat1, M. Rahbari-Sisakht. Fabrication and characterization of polyetherimide hollow fiber membrane contactor for carbon dioxide stripping from monoethanolamine solution, J. Membr. Sci. Res. 1 (2015) 118-123.
[27] R.B. Bird, W.E. Stewart, E.N. Lightfoot, Transport phenomena, 2nd ed., Jonh Wiley & Sons, Inc., New York, 2002.
[28] F.P. Incropera, D.P. DeWitt, T.L. Bergman, A.S. Lavine, Fundamentals of heat and mass transfer, 6th ed., New York, John Wiley & Sons, 2007.
[29] N.N. Li, A.G. Fane, W.S.W. Ho, T. Matsuura (Eds.), Advanced membrane technology and applications, John Wiley & Sons Inc., New York, USA, 2008.
[30] Z. Qi, E.L. Cussler, Microporous hollow fibers for gas absorption. Part 1: mass transfer in the liquid, J. Membr. Sci. 23 (1985) 321–332.
[31] G.F. Versteeg, W.P.M. van Swaaij, Solubility and diffusivity of acid gases (CO_2, N_2O) in aqueous alkanolamine solutions, J. Chem. Eng. Data 33 (1988) 29-34.
[32] S. Srisurichan, R. Jiraratananon, A.G. Fane, Mass transfer mechanisms and transport resistances in direct contact membrane distillation process, J. Membr. Sci. 277 (2006) 186-194.